Giant Influence of Clustering and Anti-Clustering of Disordered Surface Roughness on Electronic Tunneling

Yu Zhang(张羽)[1,2,4], Qingyun Zhang(张青云)[1], Youqi Ke(柯友启)[1,2,3*], and Ke Xia(夏钶)[3]

[1]*School of Physical Science and Technology, ShanghaiTech University, Shanghai 201210, China*
[2]*Shanghai Institute of Optics and Fine Mechanics, Chinese Academy of Sciences, Shanghai 201800, China*
[3]*Beijing Computational Science Research Center, Beijing 100193, China*
[4]*University of Chinese Academy of Sciences, Beijing 100049, China*

(Received 25 February 2022; accepted manuscript online 21 June 2022)

This work reveals the giant influence of spatial distribution of disordered surface roughness on electron tunneling, which is of immediate relevance to the magneto tunnel device and imaging technologies. We calculate the spin-dependent tunneling in Fe/vacuum/Fe junction with disordered surface roughness with the first-principles non-equilibrium dynamical cluster theory. It is found that, at high concentration of surface roughness, different spatial distributions, including the clustered, anti-clustered and completely random roughness characterized by Warren–Cowley parameters, present large deviations from each other in all spin channels. By changing from clustered to anti-clustered roughness, it is surprising that spin polarization of tunneling in parallel configuration (PC) can be drastically reversed from −0.52 to 0.93, while complete randomness almost eliminates the polarization. It is found that the anti-clustered roughness can dramatically quench the tunneling of minority spin in both PC and anti-PC by orders of magnitude, but significantly enhance the transmission of majority spin in PC (by as large as 40%) compared to the results of clustered roughness, presenting distinct influences of differently correlated surface roughness. The spatial correlation of disordered surface roughness can significantly modify the surface resonance of Fe minority spin.

DOI: 10.1088/0256-307X/39/8/087301

Disordered defects/impurities are often responsible for the device performance and its degradation.[1] In realistic device materials, many important defects are usually created in pairs/clusters (e.g., the anti-site defects), and possess the important clustering or anti-clustering tendencies due to their intrinsic interactions, presenting distinct distributions with different electronic states and scattering strength from the complete randomness (e.g., the clustered vacancies and anti-clustered interstitials).[2–4] However, due to great difficulties in experimental identification and theoretical treatment of spatial correlations, the crucial influence of correlated disorders remains largely unexplored in transport properties of nano-scale devices, despite the importance for a wide range of technologies. As a representative, the distribution of surface defects or roughness, determining the surface topography and states, may strongly affect the surface electron tunneling,[5–7] which is important for many technologies including the scanning tunneling microscope/spectroscope (STM/STS)[8–10] and the spin-polarized STM/STS.[11–13] The STM experiments measured the anomalous images for layered materials with different non-ideal tips,[14] and also demonstrated that the tip that provides atomic resolution often gives unpredictable and non-reproducible tunneling I–V curves,[13] illustrating important effects of tip surface structure on electron tunneling.

Surface-to-surface tunneling has been widely used and studied with the STM/STS experiments[15,16] and quantum transport simulations.[5–7,17–20] Unlike the junctions with real insulating materials, tunneling through vacuum avoids the effects of structure and atomic defects in the barrier, thus providing an ideal system for studying the critical interfacial effects on the tunneling.[21–26] The Fe/vacuum/Fe junction provides a model system for studying the physics of spin-dependent tunneling, which is the basis for magnetic tunneling junction (MTJ) possessing important applications in MRAMs. Recently, it has been revealed, by first-principles calculations with coherent potential approximation (CPA), that the completely random surface roughness can significantly change the spin-dependent tunneling in Fe/vacuum/Fe junction, drastically reducing the tunneling magnetoresistance ratio (TMR).[6,7] However, due to the implemented single-site approximation,[27,28] the CPA based quantum transport method is incapable to account for the spatial correlation of disorders, determined by the fabrication process. As a result, the influence of surface defects on tunneling is still far from being completely understood.

Very recently, some of the authors reported the first-principles non-equilibrium dynamical cluster theory (NEDCA) to provide an effective approach to include the nonlocal correlation and short-range order effects of disorders for simulating disordered nano-electronics.[29] The NEDCA in combination with highly localized exact-

*Corresponding author. Email: keyq@shanghaitech.edu.cn
© 2022 Chinese Physical Society and IOP Publishing Ltd

muffin-tin orbital (EMTO)[30–34] based density functional theory (DFT)[35,36] has been implemented into a simulation package for device materials, called SIGMAX (including both scalar- and full-relativistics).[37,38] In this work, by applying EMTO-DFT-NEDCA in scalar-relativistics, we reveal the large influence of spatial correlation of surface defects on the spin-dependent tunneling in Fe/vacuum/Fe junction.

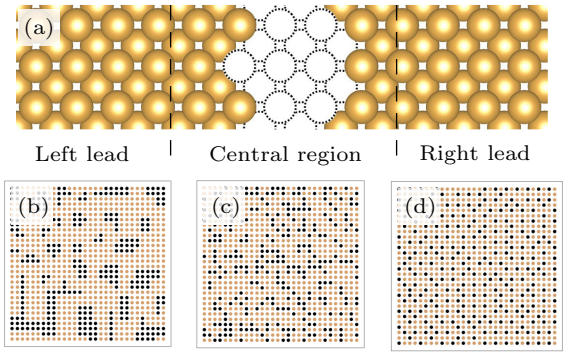

Fig. 1. (a) Atomic structure of Fe/vacuum/Fe junction in bcc (100) with surface roughness. Empty sphere is for the vacuum. (b)–(d) Illustration of the clustered, completely random and anti-clustered surface roughness with the respective $\alpha_1 = 0.5$, 0.0, -0.4 (for $x = 0.3$).

By conserving the full lattice symmetry of the device,[39–42] the NEDCA is developed to calculate the averaged Keldysh's non-equilibrium green's function (GF) in 2×2 matrix, namely

$$\bar{\boldsymbol{G}} = \begin{pmatrix} \bar{G}^{\mathcal{A}} & 0 \\ \bar{G}^{\mathcal{K}} & \bar{G}^{\mathcal{R}} \end{pmatrix},$$

where $\bar{G}^{\mathcal{A}/\mathcal{R}/\mathcal{K}}$ corresponds to the advanced/retarded and Keldysh GFs, to give the averaged non-equilibrium density and transmission in the self-consistent dynamical cluster mean-field approximation.[39–42] For example, the electron density $\bar{\rho} \sim \int d\epsilon \bar{G}^{<}(\epsilon)$, where the lesser GF $\bar{G}^{<} = \frac{1}{2}(\bar{G}^{\mathcal{A}} - \bar{G}^{\mathcal{R}} + \bar{G}^{\mathcal{K}})$, and the current is given by the Landauer–Buttiker formula

$$\bar{I} = \frac{e}{h} \int_{\mu_{\rm R}}^{\mu_{\rm L}} \overline{T}(E)[f_{\rm L}(E) - f_{\rm R}(E)]dE, \qquad (1)$$

where the averaged transmission $\overline{T} = \mathrm{Tr}[\overline{G^{\mathcal{R}} \Gamma_{\rm L} G^{\mathcal{A}} \Gamma_{\rm R}}]$, which can be rewritten as $\overline{T} = \mathrm{Tr}[-i\bar{G}^{<}\Gamma_{\rm R}]$ at zero temperature ($\Gamma_{\rm L/R}$ is the line-width function). Here, as shown in Fig. 1, for Fe/vacuum/Fe junction in bcc (100) with disordered surface roughness, we take all potential spheres' radius $2.67\mu_{\rm B}$ with $\mu_{\rm B}$ being the Bohr radius. The surface roughness is treated by alloy models $\mathrm{Fe}_x\mathrm{Va}_{1-x}$ and $\mathrm{Fe}_{1-x}\mathrm{Va}_x$ on the respective left and right surfaces, so that the averaged total barrier thickness is kept to be constant, namely 5-monolayer vacuum spheres, to avoid the dependence on barrier thickness. The disordered roughness on the two Fe surfaces is treated in two different DCA clusters, by neglecting the weak nonlocal correlation between two disordered surface layers due to the low transmission through vacuum barrier. To characterize the clustering or anti-clustering tendencies of surface defects, we use the Warren–Cowley parameters $\alpha_i = \frac{\langle \bar{\Pi}_i \rangle - q^2}{1-q^2}$ $(-1 \le \alpha_i \le 1)$, where $q = c_{\rm A} - c_{\rm B}$, $\langle \bar{\Pi}_i \rangle$ is the averaged pair-correlation function in $i^{\rm th}$ shell and $c_{\rm A/B}$ stands for the concentration of A/B atom;[43,44] $\alpha_i > 0$ presents the clustering tendency, while $\alpha_i < 0$ for the anti-clustering tendency. For complete randomness, $\alpha_i = 0$ for all i shells. Figures 1(b) and 1(c) present different roughness patterns with the respective clustering, complete random and anti-clustering tendencies for comparison. We adopt the DCA cluster size of 5×5 primitive cells and 200 disordered atomic configurations for each case. The disorder configurations of the two DCA clusters are set by exchanging the Va and Fe species. We use 50×50 $k_{\parallel}$ mesh for equilibrium and nonequilibrium (with double-energy contour)[29] electron structure, and 200×200 $k_{\parallel}$ mesh for the transmission and current. The exchange-correlation is treated in local spin density approximation.[45,46]

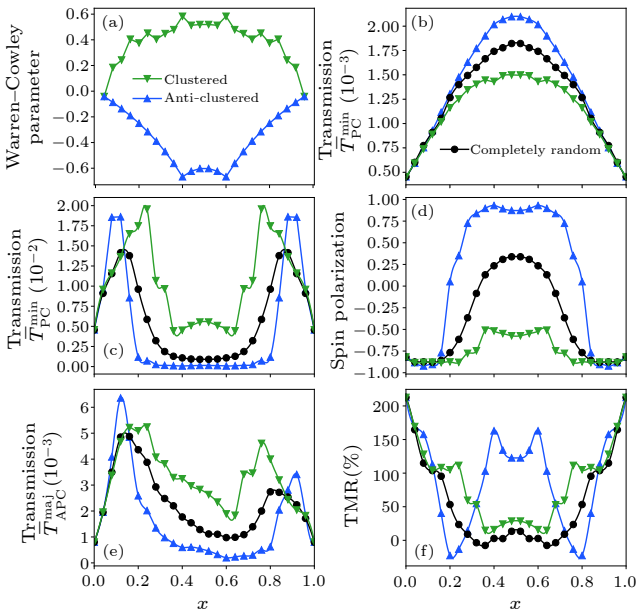

Fig. 2. (a) The Warren–Cowley parameter α_1 for maximal clustering and anti-clustering. [(b), (c)] Transmission versus disorder concentration x at $E_{\rm F}$ for $\overline{T}^{\rm maj}_{\rm PC}$ and $\overline{T}^{\rm min}_{\rm PC}$ in PC for the clustered, anti-clustered and completely random cases, respectively. (d) The spin polarization of tunneling current in PC. (e) $\overline{T}^{\rm maj}_{\rm APC}$ in APC. (f) The TMR versus x.

In Fig. 2, we investigate the transport properties (at $E_{\rm F}$) versus x for different spin channels in parallel (PC) and antiparallel (APC) configurations of Fe/vacuum/Fe MTJ with different surface roughness, including the maximal clustering (green), anti-clustering (blue) tendencies and complete randomness (black) for comparison. Figure 2(a) presents the α_1 versus x for the maximally clustered and anti-clustered cases. It should be mentioned that the clustered and anti-clustered configurations by sampling feature the short-range order, while disorder averaging with DCA accounts for the long-range disorder effects, namely the diffusive scattering. It is clear that the spatial correlation of surface roughness presents large influences on the spin dependent tunneling in Fe/vacuum/Fe. As

shown in Fig. 2(b) for PC majority spin $\overline{T}_{\rm PC}^{\rm maj}$, with increasing x, all results present significant enhancement and reach the maximum at $x = 0.5$. For example, the $\overline{T}_{\rm PC}^{\rm maj}$ results for the clustered, completely random and anti-clustered cases at $x = 0.48$ are 1.50×10^{-3}, 1.82×10^{-3} and 2.10×10^{-3}, respectively, compared to the value 0.45×10^{-3} of the clean. Moreover, by comparing the three cases, the important deviation can be found for $x\,(\text{or } 1-x) > 0.25$ due to different spatial correlation of surface roughness. For example, at $x = 0.48$, the anti-clustered and completely random roughness can importantly increase $\overline{T}_{\rm PC}^{\rm maj}$ by 40% and 22%, respectively, over the result of clustered case, illustrating the important influence of spatial correlation of surface roughness. It is clear that the clustering tendency of surface roughness can importantly suppress $\overline{T}_{\rm PC}^{\rm maj}$ in Fe/vacuum/Fe.

However, compared to $\overline{T}_{\rm PC}^{\rm maj}$, the disordered surface roughness and its spatial correlation presents very distinct influences on the $\overline{T}_{\rm PC}^{\rm min}$ as shown in Fig. 2(c). For all the three cases, $\overline{T}_{\rm PC}^{\rm min}$ presents a fast increase at the small x (or $1-x$). $\overline{T}_{\rm PC}^{\rm min}$ of the anti-clustered is increased mostly and reaches the maximum 1.85×10^{-2} at $x = 0.08$ (4.1 times of the value in the clean junction). For all three cases, the PC is dominated by $\overline{T}_{\rm PC}^{\rm min}$. As previously demonstrated, the dominance of $\overline{T}_{\rm PC}^{\rm min}$, and its large increase by small x can be attributed to the maintained Fe (100) surface resonances with nearly symmetrical barrier,[5,6] and the lifted symmetry limitation by disorder scattering.[47] However, with further increasing x (or $1-x$), the $\overline{T}_{\rm PC}^{\rm min}$ values of all three cases present quick decrease from their maximum values. In particular, for the anti-clustered case, $\overline{T}_{\rm PC}^{\rm min}$ is dramatically quenched by more than two orders of magnitude from the maximum to the minimum 7.32×10^{-5} at $x = 0.40$, while the complete randomness presents over one-order magnitude reduction (from the peak 1.4×10^{-2} at $x = 0.12$ to the minimum 9.0×10^{-4} at $x = 0.48$). Contrasting to the drastic decrease in the anti-clustered and completely random cases, the decrease in $\overline{T}_{\rm PC}^{\rm min}$ by the clustered roughness is rather limited, changing from the peak 1.96×10^{-2} at $x = 0.24$ to 5.53×10^{-3} at $x = 0.48$ (close to the value at the clean). It is clear that the large deviations among clustered, anti-clustered and completely random cases present the giant influence of spatial correlation of disordered roughness with distinct scattering mechanisms. In all the cases, the sharp drop in $\overline{T}_{\rm PC}^{\rm min}$ illustrates the fact that the surface resonance can be significantly broken or even eliminated by disordered roughness of high x at $E_{\rm F}$.[5] Figure 2(d) presents the spin polarization of the PC transmission, namely $P_{\rm PC} = (\overline{T}_{\rm PC}^{\rm maj} - \overline{T}_{\rm PC}^{\rm min})/(\overline{T}_{\rm PC}^{\rm maj} + \overline{T}_{\rm PC}^{\rm min})$. It is clear that, with increasing x, it is surprising that anti-clustered roughness drastically switches the spin polarization from $P_{\rm PC} = -0.92$ at $x = 0.08$ to $P_{\rm PC} = 0.93$ at $x = 0.4$ (maintaining high spin polarization), while the clustered case presents very limited decrease in magnitude of $P_{\rm PC}$. Rather different from other two cases, complete randomness of surface roughness (in black) eliminates $P_{\rm PC}$ with increasing x. It is clear that, at high concentration, the spatial correlations of surface roughness do present large influence on the spin polarization of tunneling current in PC.

In Fig. 2(e), we compare $\overline{T}_{\rm APC}^{\rm maj}$ of the three cases for APC (note that $\overline{T}_{\rm APC}^{\rm maj}(x) = \overline{T}_{\rm APC}^{\rm min}(1-x)$ due to the adopted device symmetry). Besides the asymmetry, $\overline{T}_{\rm APC}^{\rm maj}$ presents the similar x dependence to $\overline{T}_{\rm PC}^{\rm min}$ in Fig. 2(c), for example, the important enhancement at the small x (or $1-x$) and the important decrease at the high x for all the cases. It should be emphasized that anti-clustered roughness at high x can quickly quench $\overline{T}_{\rm APC}^{\rm maj}$ to a very small value, presenting large deviations from the other two cases (consistent with the influence found in $\overline{T}_{\rm PC}^{\rm min}$). The large deviation between the clustered and anti-clustered cases demonstrates again the important influence of spatial correlation of surface roughness on the $\overline{T}_{\rm APC}^{\rm maj}$. Our results demonstrate that the surface roughness, including both its concentration and clustering tendency, could be one of the important factors determining the imaging results in STM/STS measurements, which is highly sensitive to tip structure. We believe that, in the real STM tips, the clustered surface roughness should be more common, since the atoms prefer to stay together to lower the energy by forming more bonds. However, the detailed STM tip structure is highly dependent on the tip operating condition and the manufacturing process including the etching, annealing, etc.

In addition, in Fig. 2(f), we investigate the tunneling magnetoresistance ratio, namely $\text{TMR} = \frac{\overline{T}_{\rm PC} - \overline{T}_{\rm APC}}{\overline{T}_{\rm APC}}$. For all the cases, the TMR results present quick decrease from about 213% in the clean junction to very small values at the low x, due to the quick increase in $\overline{T}_{\rm APC}^{\rm maj}$ as shown in Fig. 2(e). However, for $0.3 < x < 0.7$, it is surprising that the anti-clustered roughness presents a large enhancement in TMR (for example, 163% at $x = 0.4$ and 123% at $x = 0.48$), in contrast to the low TMR values maintained in the clustered and completely random cases. This anomalous enhancement in TMR in the anti-clustered case is consistent with the sharp increase of spin polarization in PC shown in Fig. 2(d). Here, we have seen that the different spatial correlations of surface roughness, including the clustered, anti-clustered and completely random cases, do present rather distinct and important influences on the electron tunneling of all spin channels in Fe/vacuum/Fe junction.

In Fig. 3(a), we study the spin dependent transmission versus the Warren–Cowley parameter α_1 for $x = 0.40$, where the spatial correlation presents large influences as shown in Fig. 2. It is seen that, with increasing α_1 from -0.67 to 0.58, $\overline{T}_{\rm PC}^{\rm maj}$ presents a linear decrease from 2.02×10^{-3} to 1.43×10^{-3}. However, $\overline{T}_{\rm PC}^{\rm min}$ presents exponentially fast increase from 7.32×10^{-5} at $\alpha_1 = -0.67$ to the maximum 5.26×10^{-3} at $\alpha_1 = 0.42$ with a change of almost two order of magnitude, presenting the dramatic effects of spatial correlation of surface roughness. As a result, tunneling in PC is dominated by $\overline{T}_{\rm PC}^{\rm maj}$ for negative α_1, and by $\overline{T}_{\rm PC}^{\rm min}$ for positive α_1. For the APC, it is clear that both $\overline{T}_{\rm APC}^{\rm maj}$ and $\overline{T}_{\rm APC}^{\rm min}$ increase fast with increasing α_1. At $\alpha_1 = 0.58$, $\overline{T}_{\rm APC}^{\rm maj}$ and $\overline{T}_{\rm APC}^{\rm min}$ present the respective 4.4 and 8.6 times increase in magnitude over the values at $\alpha_1 = -0.67$. It is thus clear that controlling the spatial correlation of disordered surface roughness presents an im-

portant way to modulate the properties of tunneling. For the total transmission in PC and APC, as the spatial correlation approaches to the complete randomness, the difference between $\overline{T}_{\rm PC}$ and $\overline{T}_{\rm APC}$ becomes smaller and smaller. As an important result, as shown in Fig. 3(a), with increasing α_1 from -0.67 to 0.0, the TMR value quickly decreases from 163% to 2.8% and then slightly increases to 15.9% with further increase of α_1 to 0.58.

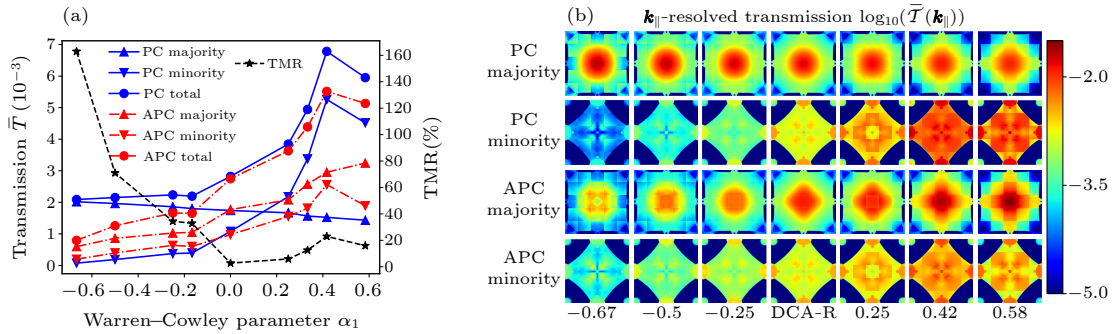

Fig. 3. (a) Transmission (for PC and APC) and TMR versus Warren–Cowley parameter α_1 for the roughness $x = 0.6$ in Fe/vacuum/Fe junction (at $E_{\rm F}$). (b) $\boldsymbol{k}_\parallel$-resolved transmission $\overline{T}(\boldsymbol{k}_\parallel)$ for different α_1 in 2D BZ for spin channels in PC and APC for $x = 0.6$ (at $E_{\rm F}$).

Figure 3(b) presents the $k_\parallel$-resolved transmission versus α_1 in different spin channels in PC and APC for $x = 0.6$ at $E_{\rm F}$. All the results present diffusive patterns due to the disorder scattering, and the 4-fold symmetry of device structure is preserved in NEDCA. It is clear that, with changing α_1 from -0.67 to 0.58, the $\overline{T}^{\rm maj}_{\rm PC}(k_\parallel)$ peak around the Γ point that dominates the transmission is gradually weakened, resulting in the linear decrease in $\overline{T}^{\rm maj}_{\rm PC}$ in Fig. 3(a). However, with increasing the α_1, $\overline{T}^{\rm min}_{\rm PC}(k_\parallel)$ presents quick enhancement, by orders of magnitude, for all $k_\parallel$ with incoming state. The large magnitude of $\overline{T}^{\rm min}_{\rm PC}(k_\parallel)$ at $\alpha_1 = 0.42$ presents a distinct tunneling mechanism compared to the negligible transmission at $\alpha_1 = -0.67$. From the highly diffusive pattern of $\overline{T}^{\rm min}_{\rm PC}(k_\parallel)$ for $\alpha_1 = 0.42$, we cannot directly evaluate the contribution of resonant tunneling, which usually presents the hot spots in clean junction, may require the shot noise.[47] For APC, $\overline{T}^{\rm maj/min}_{\rm APC}(k_\parallel)$ presents similar patterns as the PC results due to the same incoming electronic states. By increasing the clustering tendency, the important enhancement in both APC spin channels is apparent: the important increase in $\overline{T}^{\rm maj}_{\rm APC}(k_\parallel)$ is concentrated around the Γ point, and the increase in $\overline{T}^{\rm min}_{\rm APC}(k_\parallel)$ is more spread in BZ. The large contrast between the results $T^{\rm min}_{\rm PC}(k_\parallel)/T^{\rm maj/min}_{\rm APC}(k_\parallel)$ for the cases $\alpha_1 = -0.67$ and $\alpha_1 = 0.42$ reflects the fact that the Fe surface states of minority spin can be significantly modified by the spatial correlation of surface roughness.

As shown in Figs. 4(a) and 4(b), we present the transmission versus energy E ($-0.5\,{\rm eV} \le E \le 1.0\,{\rm eV}$ by shifting $E_{\rm F} = 0$) for different spin channels in the junctions with $x = 0.4$ for the three cases of $\alpha_1 = -0.67$, 0.0, 0.58, and compare with the result of the clean junction. In the inset of Fig. 4(a) for $\overline{T}^{\rm maj}_{\rm PC}$, all the cases present much larger transmission than the clean result, and quite fast increase with increasing E. It is clear that, compared to the completely random case, the anti-clustered roughness always enhances the transmission in the wide range of E, while the clustered roughness suppresses the result. However, large deviation between different cases is found in $\overline{T}^{\rm min}_{\rm PC}$ shown in Fig. 4(a), illustrating the important influence of spatial correlation of roughness. For example, the anti-clustered case presents a sharp resonant peak with a maximum $\overline{T}^{\rm min}_{\rm PC} = 7.6 \times 10^{-2}$ at $E = 0.7\,{\rm eV}$, while the peak in completely random case, with a maximum $\overline{T}^{\rm min}_{\rm PC} = 4.5 \times 10^{-2}$ at $E = 0.6\,{\rm eV}$, is more spread in energy. However, the clustered roughness presents doubles peaks (with maximum 3.5×10^{-2} at $E = 0.6\,{\rm eV}$, and the second 2.7×10^{-2} at $E = 0.2\,{\rm eV}$ close to $E_{\rm F}$), and thus presents high transmission probability in a wide range of energy. As an important result of the spread peak close to $E_{\rm F}$, the clustered $\overline{T}^{\rm min}_{\rm PC}$ is much larger than the other two cases, as shown in Figs. 2(c) and 3. It should be mentioned that the peaks in $T^{\rm min}_{\rm PC}$ are associated with the surface resonance of Fe minority spin. By comparing with the result of the clean (with the resonant peak at $E = -0.2\,{\rm eV}$), we can see that, by controlling both concentration and spatial correlation of surface roughness, the surface resonance of Fe minority spin can be significantly modified to present distinct $T(E)$, which may also influence the related tunneling anisotropic magnetoresistance.[26] For APC, similar results to $\overline{T}^{\rm min}_{\rm PC}$ can be found in both spin channels, as shown in Fig. 4(b) and the inset, for example, the presence of a second peak close to $E_{\rm F}$ in the clustered case. It is clear that, by changing the clustering to anti-clustering tendencies, the peak is importantly enhanced and shifted to higher energy away from $E_{\rm F}$, significantly reducing the transmission at $E_{\rm F}$ for $\overline{T}^{\rm min}_{\rm PC}$ and $\overline{T}^{\rm maj/min}_{\rm APC}$.

To investigate the important influence of spatial correlation of surface roughness on the far-from-equilibrium properties of Fe/vacuum/Fe junctions, we performed the self-consistent EMTO-DFT-NEDCA calculation of the electronic structure under finite bias, and plot the spin-dependent I–V curves in Figs. 4(c)–4(d) for the three disordered roughness cases same as in Figs. 4(a)–4(b). It is seen that, in Fig. 4(c) inset, $\overline{I}^{\rm maj}_{\rm PC}$ of all cases present a fast increase with bias V, consistent with the monotonic behavior in $\overline{T}^{\rm maj}_{\rm PC}(E)$ shown in Fig. 4(a) inset. However,

for $\overline{I}_{\rm PC}^{\rm min}$ shown in Fig. 4(c), $\overline{I}_{\rm PC}^{\rm min}$ of the clustered case (in green) presents a significant increase at low bias voltage attributed to the second resonant peak in $\overline{T}_{\rm PC}^{\rm min}(E)$ close to $E_{\rm F}$ [as shown in Fig. 4(a)], while the other two cases present marginal increase. With further increase of the bias, all the cases present fast increases in $\overline{I}_{\rm PC}^{\rm min}$ due to large resonance peaks at high energy as shown in Fig. 4(a). As shown in Fig. 4(d) inset for $\overline{I}_{\rm APC}^{\rm maj}$, all the I–V curves present rather monotonic and quick increase with the clustered case increased most apparently. Interestingly, different from $\overline{I}_{\rm APC}^{\rm min}$ at low bias, $\overline{I}_{\rm PC}^{\rm min}$ and $\overline{I}_{\rm APC}^{\rm maj}$, $\overline{I}_{\rm APC}^{\rm min}$ at high bias for anti-clustered and complete random cases are dramatically enhanced over the result of clustered case, due to the large resonance in minority spin as shown in Fig. 4(b). In addition, the bias dependence of TMR for all the three cases is shown in Fig. 4(d). The remarkable TMR of anti-clustered case is quickly decreased from 163% at zero bias to −33% at $V_{\rm b} = 0.8\,{\rm V}$, while the other two cases maintain small TMR values. We can see that the three cases in Fig. 4 present distinct bias dependences in all spin channels, presenting the important influence of spatial correlation of surface roughness on the tunneling under finite bias.

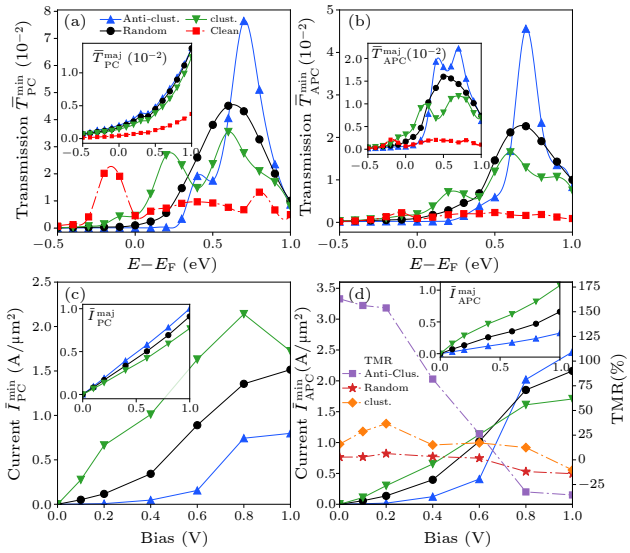

Fig. 4. [(a), (b)] Transmission versus energy for PC (a) and APC (b) for majority (insets) and minority spin channels at zero bias. [(c), (d)] Spin-polarized currents versus bias for PC (c) and APC (d) for majority (insets) and minority spin channels. Right axis in (d): TMR versus bias.

In summary, we have revealed the giant influence of spatial distribution of disordered surface roughness on electronic tunneling. By utilizing the EMTO-DFT-NEDCA first-principles quantum transport method, we calculate the spin-dependent tunneling in Fe/vacuum/Fe junction with disordered surface roughness. It is found that the anti-clustered roughness can drastically quench the tunneling of minority spin in PC and APC by orders of magnitude, but significantly enhance the transmission of majority spin in PC by about 40% compared to the result of clustered roughness. As a result, the spin polarization of tunneling in PC can be dramatically switched from −0.52 to 0.93 by changing disordered roughness from the clustered to anti-clustered, while the complete randomness could eliminate the polarization, presenting the large effects of spatial correlation of surface roughness. The spatial correlation of surface roughness can significantly modify the surface resonance of the Fe minority spin. Our results demonstrate that controlling the spatial distribution of disordered surface roughness can provide an important way to modulate the electronic tunneling properties.

Acknowledgments. Y. Ke acknowledges financial support from the National Natural Science Foundation of China (Grant No. 11874265) and Shanghaitech Startup. K. Xia is supported by the National Key Research and Development Program of China (Grant Nos. 2017YFA0303300 and 2018YFB0407601), the National Natural Science Foundation of China (Grant Nos. 11734004 and 21421003). The authors thank the HPC platform of ShanghaiTech University for providing computational facility.

References

[1] Koenraad P M and Flatté M E 2011 *Nat. Mater.* **10** 91
[2] Wei S H, Ferreira L G, Bernard J E and Zunger A 1990 *Phys. Rev. B* **42** 9622
[3] Allnatt A R and Lidiard A B 1993 *Imperfections in Solids* (Cambridge: Cambridge University Press) p 50
[4] Zunger A, Wei S H, Ferreira L G and Bernard J E 1990 *Phys. Rev. Lett.* **65** 353
[5] Wunnicke O, Papanikolaou N, Zeller R, Dederichs P H, Drchal V and Kudrnovský J 2002 *Phys. Rev. B* **65** 064425
[6] Xu P X, Karpan V M, Xia K, Zwierzycki M, Marushchenko I and Kelly P J 2006 *Phys. Rev. B* **73** 180402(R)
[7] Ke Y, Xia K and Guo H 2008 *Phys. Rev. Lett.* **100** 166805
[8] Binnig G, Rohrer H, Gerber C and Weibel E 1982 *Appl. Phys. Lett.* **40** 178
[9] Binnig G, Rohrer H, Gerber C and Weibel E 1982 *Phys. Rev. Lett.* **49** 57
[10] Binnig G, Frank K H, Fuchs H, Garcia N, Reihl B, Rohrer H, Salvan F and Williams A R 1985 *Phys. Rev. Lett.* **55** 991
[11] Wiesendanger R, Güntherodt H J, Güntherodt G, Gambino R J and Ruf R 1990 *Phys. Rev. Lett.* **65** 247
[12] Bode M, Getzlaff M and Wiesendanger R 1998 *Phys. Rev. Lett.* **81** 4256
[13] Chen C J 1993 *Introduction to Scanning Tunneling Microscopy* (Oxford: Oxford University Press)
[14] Mizes H A, Park S I and Harrison W A 1987 *Phys. Rev. B* **36** 4491
[15] Bischoff M M J, Konvicka C, Quinn A J, Schmid M, Redinger J, Podloucky R, Varga P and van Kempen H 2001 *Phys. Rev. Lett.* **86** 2396
[16] Takahashi Y, Miyamachi T, Ienaga K, Kawamura N, Ernst A and Komori F 2016 *Phys. Rev. Lett.* **116** 056802
[17] Tsymbal E Y, Mryasov O N and LeClair P R 2003 *J. Phys.: Condens. Matter* **15** R109
[18] Zhang X G and Butler W H 2003 *J. Phys.: Condens. Matter* **15** R1603
[19] Ke Y, Xia K and Guo H 2010 *Phys. Rev. Lett.* **105** 236801
[20] Butler W H, Zhang X G, Schulthess T C and MacLaren J M 2001 *Phys. Rev. B* **63** 092402
[21] Stroscio J A, Pierce D T, Davies A, Celotta R J and Weinert M 1995 *Phys. Rev. Lett.* **75** 2960
[22] Alvarado S F 1995 *Phys. Rev. Lett.* **75** 513
[23] Okuno S N, Kishi T and Tanaka K 2002 *Phys. Rev. Lett.* **88** 066803

[24] Ding H F, Wulfhekel W, Henk J, Bruno P and Kirschner J 2003 *Phys. Rev. Lett.* **90** 116603

[25] Bischoff M M J, Yamada T K, Fang C M, de Groot R A and van Kempen H 2003 *Phys. Rev. B* **68** 045422

[26] Chantis A N, Belashchenko K D, Tsymbal E Y and van Schilfgaarde M 2007 *Phys. Rev. Lett.* **98** 046601

[27] Soven P 1967 *Phys. Rev.* **156** 809

[28] Taylor D W 1967 *Phys. Rev.* **156** 1017

[29] Zhang Y, Zhai J, Chen Z, Zhang Q and Ke Y 2021 *Phys. Rev. B* **104** 115412

[30] Andersen O K, Jepsen O and Krier G 1995 *Exact Muffin-Tin Orbital Theory*, in *Lectures on Methods of Electronic Structure Calculations* (Singerpore: World Scientific) pp 63–124

[31] Andersen O K, Arcangeli C, Tank R W, Saha-Dasgupta T, Krier G, Jepsen O and Dasgupta I 1997 *MRS Online Proc. Libr.* **491** 3

[32] Vitos L, Skriver H L, Johansson B and Kollár J 2000 *Comput. Mater. Sci.* **18** 24

[33] Vitos L, Abrikosov I A and Johansson B 2001 *Phys. Rev. Lett.* **87** 156401

[34] Vitos L 2007 *Computational Quantum Mechanics for Materials Engineers: The EMTO Method and Applications* (London: Springer)

[35] Hohenberg P and Kohn W 1964 *Phys. Rev.* **136** B864

[36] Kohn W and Sham L J 1965 *Phys. Rev.* **140** A1133

[37] Zhang Q, Yan J, Zhang Y and Ke Y 2019 *Phys. Rev. B* **100** 075134

[38] Chen Z, Zhang Q, Zhang Y, Wang L, Sang M and Ke Y 2020 *Phys. Rev. B* **102** 035405

[39] Hettler M H, Tahvildar-Zadeh A N, Jarrell M, Pruschke T and Krishnamurthy H R 1998 *Phys. Rev. B* **58** R7475

[40] Hettler M H, Mukherjee M, Jarrell M and Krishnamurthy H R 2000 *Phys. Rev. B* **61** 12739

[41] Jarrell M and Krishnamurthy H R 2001 *Phys. Rev. B* **63** 125102

[42] Maier T A, Jarrell M, Pruschke T and Hettler M 2005 *Rev. Mod. Phys.* **77** 1027

[43] Cowley J M 1950 *J. Appl. Phys.* **21** 24

[44] Wolverton C, Ozoliņš V and Zunger A 1998 *Phys. Rev. B* **57** 4332

[45] Ceperley D M and Alder B J 1980 *Phys. Rev. Lett.* **45** 566

[46] Perdew J P and Zunger A 1981 *Phys. Rev. B* **23** 5048

[47] Yan J, Wang S, Xia K and Ke Y 2018 *Phys. Rev. B* **97** 014404